LARGE-SCALE MANIPULATION OF A TURBULENT BOUNDARY LAYER BY MEANS OF A 2D SYNTHETIC JET

G. M. Di Cicca*, G. Iuso*
***DIASP, Politecnico di Torino (ITALY)**

Keywords: *PIV, Synthetic Jet, Turbulent Boundary Layer*

Abstract

Large-scale manipulation of a turbulent boundary layer has been obtained by using a yawed quasi-2D synthetic jet interacting with the mean flow. Measurements were taken by means of Digital Particle Image Velocimetry. Images were recorded in planes perpendicular to the wall and aligned with the main flow, in planes perpendicular to the wall and to the main flow and in planes parallel to the wall. For appropriate slit orientations and forcing frequencies specific zones of the near wall region showed a reduced turbulent activity. A reduction of Q2 events detected in the region closer to the wall is observed. Moreover, VISA analysis and the correlation function computed for the longitudinal component of the velocity showed the presence of more fragmented coherent structures.

1 Introduction

The structure and regeneration mechanisms of turbulence in wall bounded flows can be heavily modified when an external forcing is present. In particular, it has been demonstrated that large-scale control strategies can produce huge modifications of the flow organization and turbulence activity even if the forcing is weak. Marked reduction in turbulence fluctuations can be obtained superimposing large-scale longitudinal counter-rotating vortices over a turbulent channel flow ([5], [7]) or a turbulent boundary layer [4]. This reduction of turbulence activity was explained through a direct reference to the turbulent regeneration mechanisms based on the instability of the low speed streaks and to the mechanisms of momentum transport due to the large-scale vortical motions in the direction of the wall for the inflow section and away from the wall for the outflow section. In the past, large-scale longitudinal vortical structures embedded in a wall turbulent flow were generated using an oriented rectangular continuous or synthetic yet interacting with the main flow. Zhang and Collins [9] examined the development of a longitudinal vortex produced as a result of the interaction between a rectangular continuous jet and a two-dimensional flat plate boundary layer. They observed that the longitudinal vortex produces momentum transfer in the spanwise direction and transverse direction. Also, the flow appears to be characterized by a vorticity peak located underneath the center of the vortex. An experimental study on streamwise vortices generated by a rectangular continuous jet in an otherwise flat plate turbulent boundary layer was carried out by Zhang [8]. The results showed that the optimal skew angle for the vortex production is equal to 45° and the circulation level of the generated vortex linearly decreases moving downstream. Bridges and Smith [2] investigated experimentally the influence of a 2D orifice orientation on the interaction between a synthetic jet and a turbulent boundary layer. According to the yaw angle of the synthetic jet slit, the presence of a counter-rotating vortex pair or a single vortex was observed in the boundary layer. Elevated streamwise turbulence intensity levels were found in the boundary layer for all yaw angles investigated.

The present paper examines the effects of the large-scale streamwise vortices, produced by

the interaction between a flat plate turbulent boundary layer and a yawed quasi-2D synthetic jet, on the turbulence structure.

2 Experimental set-up

A closed loop water tunnel was used in order to carry out the experiment (figure 1). Measurements were taken over a flat plate 2050mm long, with imposed transition at the leading edge (figure 2a). The actuator system (figure 2c) was constituted by a micro-cylinder and a stepper motor produced by a cam the sinusoidal oscillation of the piston. The flow was seeded with spherical solid particles, 2 microns nominal diameter. PIV images were captured by a digital video camera PCO Sensicam characterized by a resolution equal to 1280x1024 pixels and a Nd-YAG laser source with 200mJ of energy per pulse provided the double-pulsed light sheet. The investigation has been performed capturing images in planes (x,y) perpendicular to the wall and aligned with the main flow, in planes (y,z) perpendicular to the wall and to the main flow and in planes (x,z) parallel to the wall. The image analysis was performed using cross-correlation based algorithms. In the last iteration interrogation areas of 32x32 pixels were 50% overlapped.

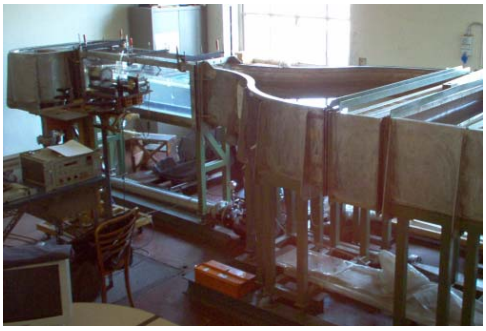

Fig. 1. Closed loop water tunnel.

The natural turbulent boundary layer at the injection section was characterized by a Reynolds number based on the momentum thickness equal to about 1000 and a thickness δ=30mm. The reduced actuation frequency $\tilde{f} = f \cdot \delta / U_e$ was kept constant at 0.27 and the velocity ratio $R = U_0 / U_e$ was about 0.5. The velocity U_0 is defined as $U_0 = \frac{1}{T}\int_0^{T/2} u_0(t)dt$ where $u_0(t)$ is the instantaneous velocity at the exit plane of the jet and $T = 1/f$ is the period of oscillation; U_e is the boundary layer external velocity. The Reynolds number of the synthetic jet, based on the velocity U_0 and the slit width h, was about 900. The non-dimensional stroke-length L_0/h was equal to 10.9, corresponding to a Strouhal number equal to 0.092. The stroke-length L_0 is defined as $L_0 = \int_0^{T/2} u_0(t)dt$.

The length and the width of the synthetic jet slit are 123mm and 5mm respectively. The slit was situated 1503mm downstream the leading-edge of the flat plate. The origin of the coordinates axes was located at the centre of the slit, as shown in figure 2a. Positive yaw angles β are measured counter-clockwise when the slit is viewed from above (figure 2b).

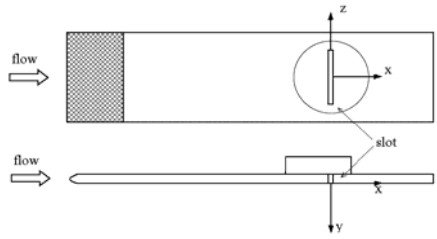

a)

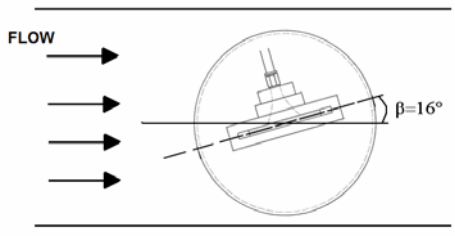

b)

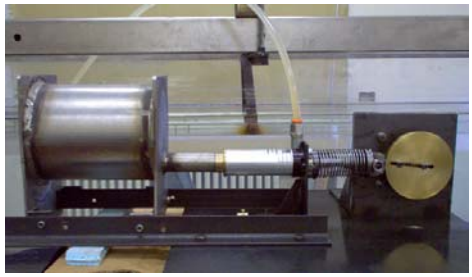

c)

Fig. 2. a) Test model; b) Close-up sketch of the synthetic jet slit; c) Actuator system.

3 Flow statistics

Measurements in a transversal plane (y,z) at a streamwise distance x/δ=3.7 from the centre of the slit have been performed for a reduced actuation frequency $\tilde{f} = 0.27$ and an orifice yaw angle β=16°.

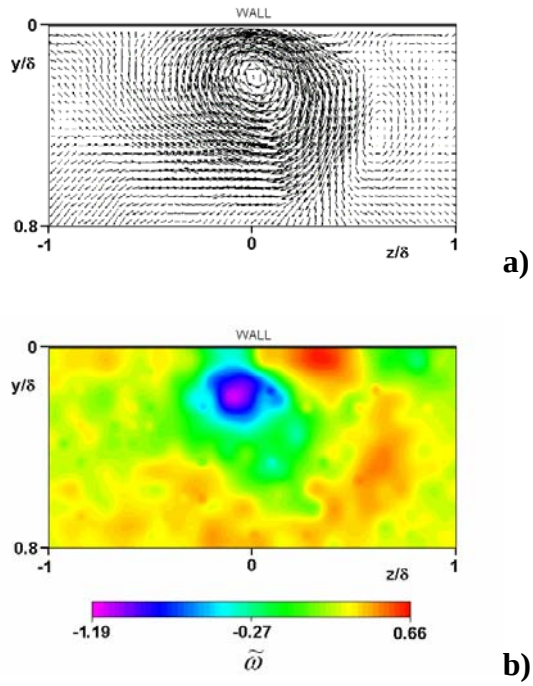

Fig. 3. a) Mean velocity vector field. b) Streamwise mean vorticity colour map. β=16° .

A rear view of the mean velocity vector field is reported in figure 3a. The wall is located at y=0. It is clearly visible a counter-rotating vortex pair. The result of the interaction between the synthetic jet and the boundary layer is the formation of a strong vortical structure with clockwise rotation (looking upstream) and a very weak vortical structure with an opposite rotation. The rotation of the vortex pair tends to sweep high-momentum fluid towards the wall in the down-flow region and to push low-momentum fluid away from the wall in the up-flow region. Cross-flow regions, where the flow direction is tangent to the wall, can be observed under the vortex axes.

Figure 3b shows the colour map of the nondimensional streamwise mean vorticity component ($\tilde{\omega} = \overline{\omega}_x \delta / U_e$). The negative peak value in the left vortex core is equal to about -1.13. A region (centered in y/δ=0.05 and z/δ=0.3) of positive streamwise vorticity, induced by the clockwise vortex, is visible close to the wall. The maximum vorticity value in this region is equal to 0.56. The maximum positive value in the counter-clockwise vortical structure core is equal to 0.33.

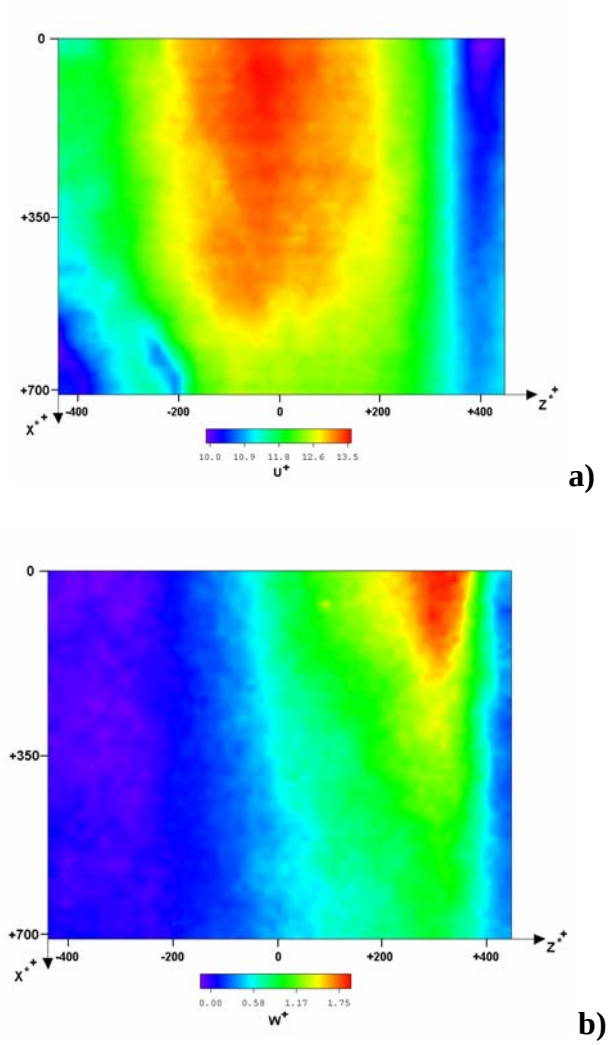

Fig. 4. a) Map of streamwise mean velocity component U. b) Map of spanwise mean velocity component W. Manipulated flow. $y^+ \approx 20$.

The colour maps of the streamwise and the spanwise mean velocity component in a plane parallel to the wall located at $y^+ \approx 20$ for the manipulated case are shown in figure 4a and 4b respectively. The center of the maps is positioned x/δ=3.7 downstream from the centre of the slit. The observed area spans about 700 wall units in the streamwise direction and 890

wall units in the spanwise direction. The main flow is directed towards positive x*. Figure 4a clearly shows three zones with an almost constant momentum. These zones are located in correspondence of the up-flow, cross-flow and down-flow regions produced by the presence of large-scale streamwise vortices. It is interesting to observe that the intensity of these zones diminishes moving downstream. An even more marked decrease of flow velocities is evident for the spanwise component. This should be probably related to the weakening of large-scale streamwise vortices due to vorticity diffusion.

Measurements have been also performed in the planes (x,y) for $z/\delta \approx -0.17$, 0 and 0.5; these positions are representative of the down-flow, cross-flow and up-flow regions respectively. The mean streamwise velocity profiles measured at a streamwise distance $x/\delta=3.7$ and made nondimensional using the friction velocity of the natural case, are reported in figure 5. The velocity profile of the natural case and the law of the wall for a canonical turbulent boundary layer are also shown on the plot for comparison. In the up-flow region the velocities are heavily reduced (up to 22% at $y^+ \approx 50$) for all the y positions. The cross-flow region exhibits a much less evident reduction of velocities respect to the the up-flow region. In the down-flow region for y^+ up to about 60 it is visible a slight increasing of the mean velocities; for $y^+ > 60$ a reduction of the mean velocities is observable, analogously to the up-flow and cross-flow regions.

This distortion of the velocity profiles is consistent with the fact that the counter-rotating vortex pair sweeps high-momentum fluid towards the wall in the down-flow region and pushes low-momentum fluid away from the wall in the up-flow region.

Figure 6 shows the variance of the streamwise velocity component for the natural and the manipulated flow. The squared friction velocity of the natural case is used to make dimensionless the variance values. The distribution of $(u'^+)^2$ is deeply modified by the manipulation and elevated streamwise fluctuations, with values much higher than those pertaining to the natural case, are observable all over the distances from the wall but with the exception of the zone closer to the wall. This increase in fluctuations is due primarily to the presence of the synthetic jet that also determines a huge increasing of the wall normal fluctuations and of the Reynolds shear stresses (these distributions are not shown here; for further details see [3]). However, in the up-flow and cross-flow regions, reductions up to 19% can be observed in the zone up to about $y^+=30$.

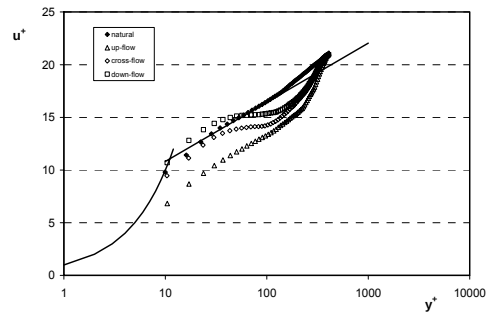

Fig. 5. Mean streamwise velocity profiles; diamonds: unmanipulated flow; open triangles, diamonds, squares: manipulated flow at $z/\delta \approx -0.17$ (down-flow), $z/\delta \approx 0$ (cross-flow) and $z/\delta \approx 0.5$ (up-flow) respectively. Solid line: law of the wall; $x/\delta=3.7$.

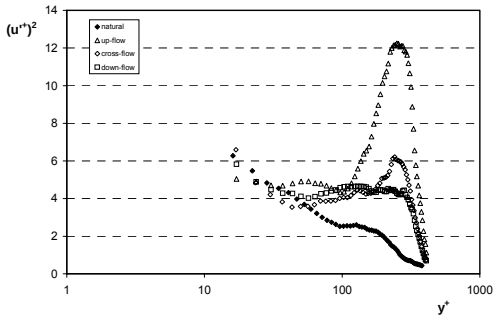

Fig. 6. Variance of the streamwise velocity component; diamonds: unmanipulated flow; open triangles, diamonds, squares: manipulated flow at $z/\delta \approx -0.17$ (down-flow), $z/\delta \approx 0$ (cross-flow) and $z/\delta \approx 0.5$ (up-flow) respectively. $x/\delta=3.7$.

3 Coherent structure analysis

Figures 7a and 7b show the maps of instantaneous longitudinal fluctuating component of the velocity in the xz plane (parallel to the wall) respectively in the case of uncontrolled and forced flow, for a distance of about 20 wall units (corresponding to $y/\delta=0.04$). The dimensions of the flow field investigated in these planes are about 700 wall units in the

streamwise direction and about 890 wall units in the spanwise direction. Looking at these instantaneous flow fields, the near wall streaky structure in the forced case seems to be strongly modified by the presence of the forcing. In particular, the streaks show a more fragmented pattern.

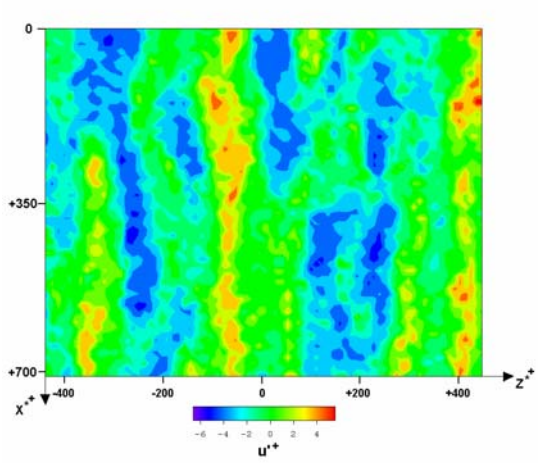

a)

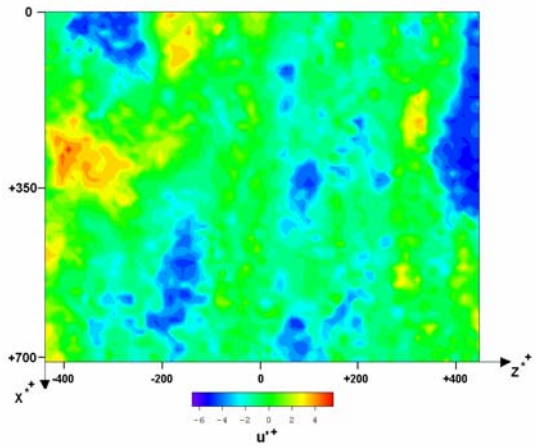

b)

Fig. 7. Maps of instantaneous longitudinal fluctuating component of the velocity. a) Natural flow; b) Forced flow (β=16°, $\tilde{f} = 0.27$).

The presence of more fragmented coherent structures in the region closer to the wall can be also deduced from the correlation fuction R_{uu} computed for the longitudinal component of the velocity. Figure 8 shows the spatial correlation function R_{uu} in a plane (x,z) at a distance from the wall equal to y^+=20. The global organization of the flow is affected by the forcing. In fact, in the manipulated case, the R_{uu} values are always lower respect to the natural case. A reduction of the longitudinal integral scale, for all the spanwise positions investigated, is observable and can be attributed to the presence of more fragmented streaks in the manipulated flow as previously shown in figure 7b. In particular the cross-flow region is characterized by the lowest value of the longitudinal integral scale.

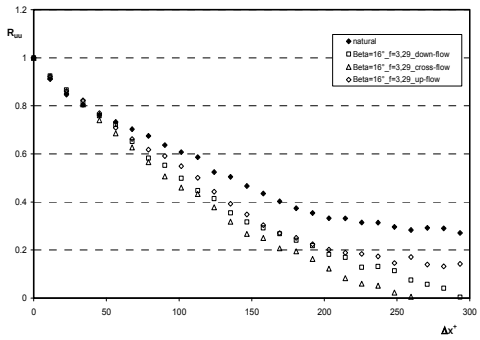

Fig. 8. Spatial autocorrelation R_{uu} along the streamwise coordinate at a distance from the wall y^+=20.

The number of Q2 events per unit length, N_q , at y^+=16, and for a threshold constant $H = 1$ is reported in table 1. A Q2 event is detected when $|uv| > Hu_{RMS}v_{RMS}$ with $u < 0$ and $v > 0$ (see [1]). u_{RMS} and v_{RMS} are the actual root mean square values of the velocity fluctuations u and v. The frequency of Q2 events for the manipulated flow is consistently diminished in the up-flow (–62%), cross-flow (–63%) and down-flow (–44%) regions respect to the natural case.

$N_q\delta$ Natural	$N_q\delta$ Manipulated (up-flow)	$N_q\delta$ Manipulated (cross-flow)	$N_q\delta$ Manipulated (down-flow)
9.60E-01	3.69E-01	3.57E-01	5.36E-01

Table 1. Number of Q2 events detected per unit length at y^+=16.

VISA technique [6] has been also applied in order to observe the effect of the manipulation on the spatial frequency of occurrence of internal shear layer events N. The non-dimensional frequency of the occurring accelerated (decelerated in space) events N^+, computed at y^+=16, for a short integration length L^+=200 and a threshold constant K=1, is reported in table 2. The short integration length

is scaled with respect to the standard boundary layer inner variables.

N^+ Natural	N^+ Manipulated (upflow)	N^+ Manipulated (crossflow)	N^+ Manipulated (downflow)
3.3E-04	12.0E-04	12.6E-04	11.9E-04

Table 2. Frequency of occurrence of VISA events at y^+=16; k=1, L^+=200, du/dx<0

In the case of the natural boundary layer the non-dimensional frequency N^+ is equal to 3.3E-04. If we look at table 1 we can observe an overall increase of the frequency of events for all the spanwise positions investigated, with respect to the natural boundary layer case. This fact can be related to the presence of more fragmented coherent structures as previously observed.

Conclusions

The interaction between a flat plate turbulent boundary layer and a 2D synthetic jet has been investigated. The interaction gives rise to large-scale longitudinal vortices.

The mean velocity profiles are distorted by the presence of the large scale longitudinal vortical structure that sweeps high momentum fluid towards the wall in the down-flow region and ejects low momentum fluid away from the wall in the up-flow region.

An overall increase of velocity fluctuations is observed for the up-flow and the down-flow regions with the exception of the very near wall zone. The huge increase of fluctuations is due to the effect of the periodic motion of the forced flow field imposed by the actuator.

Although the analysis of *uv*-quadrant method seems to evidence a reduction of Q2 events detected in the region closer to the wall, VISA technique indicates an increase in the bursting frequency. Also, the analysis of the autocorrelation function computed for the longitudinal component of the velocity evidenced flow features that can be associated with the presence of more fragmented flow structures.

Acknowledgements

The authors wish to thank Mr. A. G. Gismondi and Mr. G. Accardi, students, for their help in taking the measurements. This work was supported by grants from MIUR, INRIM and Regione Piemonte Research Project E40 (Bando 2004).

References

[1] Alfredsson P H and Johansson A V. On the Detection of Turbulence-Generating Events. *J. Fluid Mech,* vol. 139, pp. 325-345, 1984.

[2] Bridges A and Smith D R. Influence of Orifice Orientation on a Synthetic Jet – Boundary Layer Interaction. *AIAA Journal*, 41, No.12, December 2003.

[3] Di Cicca G M and Iuso G. On a Yawed Synthetic Jet – Turbulent Boundary Layer Interaction. *Proceedings of the 6th International Symposium on Particle Image Velocimetry (PIV'05)*, Pasadena, California, USA, September 21-23, 2005.

[4] Di Cicca G M, Iuso G, Spazzini P G and Onorato M. PIV Study of the Influence of Large-Scale Streamwise Vortices on a Turbulent Boundary Layer. *Experiments in Fluids*, vol. 33, pp. 663-669, 2002.

[5] Iuso G and Di Cicca G M. Interaction of Synthetic Jets with a Fully Developed Turbulent Channel Flow. *Journal of Turbulence*, vol. 8, No. 11, pp. 1-33, 2007.

[6] Kim J. Turbulence Structures Associated with the Bursting Event. *Phys. Fluids*, vol. 28(1), pp. 52-58, 1985.

[7] Schoppa W and Hussain F. Coherent Structure Generation in Near-Wall Turbulence. *J. Fluid Mech,* vol. 453, pp. 57-, 2002.

[8] Zhang X. An Inclined Rectangular Jet in a Turbulent Boundary Layer-Vortex Flow. *Experiments in Fluids*, vol. 28, pp. 344-354, 2000.

[9] Zhang X and Collins M W. Measurements of a Longitudinal Vortex Generated by a Rectangular Jet in a Turbulent Boundary Layer. *Phys. Fluids*, vol. 9(6), pp. 1665-1673, 1997

Copyright Statement